

# Plasmonic Transition via Interparticle Coupling of Au@Ag Core-Shell Nanostructures Sheathed in Double Hydrophilic Block Copolymer for High-Performance Polymer Solar Cell

*Eunyong Seo,<sup>1‡</sup> Seo-Jin Ko,<sup>1‡</sup> Sa Hoon Min,<sup>1</sup> Jin Young Kim,<sup>1\*</sup> and Byeong-Su Kim<sup>1,2\*</sup>*

<sup>1</sup>Department of Energy Engineering, Ulsan National Institute of Science and Technology  
(UNIST), Ulsan 689-798, Korea

<sup>2</sup>Department of Chemistry, Ulsan National Institute of Science and Technology (UNIST),  
Ulsan 689-798, Korea

## **The theoretical chain length of PEO block on Au@DHBC NPs.**

Mean square end-to-end length for PEO chain with restricted bond angle<sup>1</sup> is

$$\langle h^2 \rangle = Nb^2 \frac{1 + \cos\theta}{1 - \cos\theta}$$

Where  $h^2$  is mean square end-to-end length,  $N$  is the number of repeat units,  $b$  is the statistical segment length and  $\theta$  is the angle for the freely rotating of PEO blocks.

$$h^2 = 114 \times (0.6 \text{ nm})^2 \times \left( \frac{1 + \cos 70^\circ}{1 - \cos 70^\circ} \right) = 83.7 \text{ nm}^2$$

(C-C-O bond angle = 110°,  $\theta = 180^\circ - \text{bond angle}(\circ) = 180^\circ - 110^\circ = 70^\circ$ )

Therefore, the average length of PEO blocks,  $\langle h \rangle$ , is 9.1 nm.

## Experimental Section

**Materials.** Gold(III) chloride trihydrate ( $\text{HAuCl}_4 \cdot 3\text{H}_2\text{O}$ ), silver nitrate ( $\text{AgNO}_3$ ), sodium citrate tribasic dehydrate, cetyltrimethylammonium bromide (CTAB), L-ascorbic acid (AA), and Sodium borohydride ( $\text{NaBH}_4$ ) from Sigma-Aldrich were used without further purification.

**Synthesis of citrate-capped Au NPs.** Au NPs are prepared by a modified process developed by Murphy and coworkers.<sup>2</sup> The Au NPs with an average diameter of below 5 nm is first synthesized to use as a seed. Typically, 0.05 mL of 0.0667 M  $\text{HAuCl}_4$  and 0.05 mL of 0.1 M citrate were dissolved under vigorous stirring in 20 mL of aqueous solution, followed by the addition of 0.6 mL of 0.1 M  $\text{NaBH}_4$ . After a few seconds, the solution turned to transparent red, indicating the formation of spherical Au NPs. The Au solution should be used as seeds for the growth of NPs within 2-5 h after the preparation because of the stability of NPs in solution.

For the controlling the size of NPs, 200 mL of water containing  $2.5 \times 10^{-3}$  M  $\text{HAuCl}_4$  and 6 g of CTAB is prepared at 50 °C to use as a growth solution. In first growth step, 9.0 mL of growth solution was mixed with 0.5 mL of 0.1 M ascorbic acid (AA). Next, 1.0 mL of Au seed solution was added while stirring for 10 min. In the second step, 10.0 mL of growth solution was mixed with 0.556 mL of 0.1 M AA, and then all solution obtained from first growth step was added into the growth solution under stirring. After the second step was repeated once, the resulting solution was centrifuged to remove excess surfactant, followed by redispersion in water.

## Supporting Information

**Synthesis of citrate-capped Ag NPs.** Typically, 0.05 mL of 0.1 M AgNO<sub>3</sub> and 0.10 ml of 0.1 M citrate were dissolved under vigorous stirring in 20 ml of aqueous solution, and then 0.10 mL of 0.1 M NaBH<sub>4</sub> is added into solution. The solution immediately turned yellow, indicating the formation of Ag seeds. The Ag solution should be used as seeds for the growth of NPs within 2-5 h after the preparation because of the stability of NPs in solution.

For the growth of NPs, a 20 mL of water containing  $2.5 \times 10^{-3}$  M AgNO<sub>3</sub> and 50.0 mg of CTAB is prepared to use as a growth solution. A 9.0 mL of growth solution was mixed with 0.5 mL of 0.1 M AA, and then, 1.0 mL of Ag seed solution was added into the suspension under vigorous stirring for 10 min. Thereafter, additional 10 mL of growth solution is mixed with injection rate of 0.1 mL/min. After the growth step, the resulting solution was centrifuged to remove excess surfactant, followed by redispersion in water.

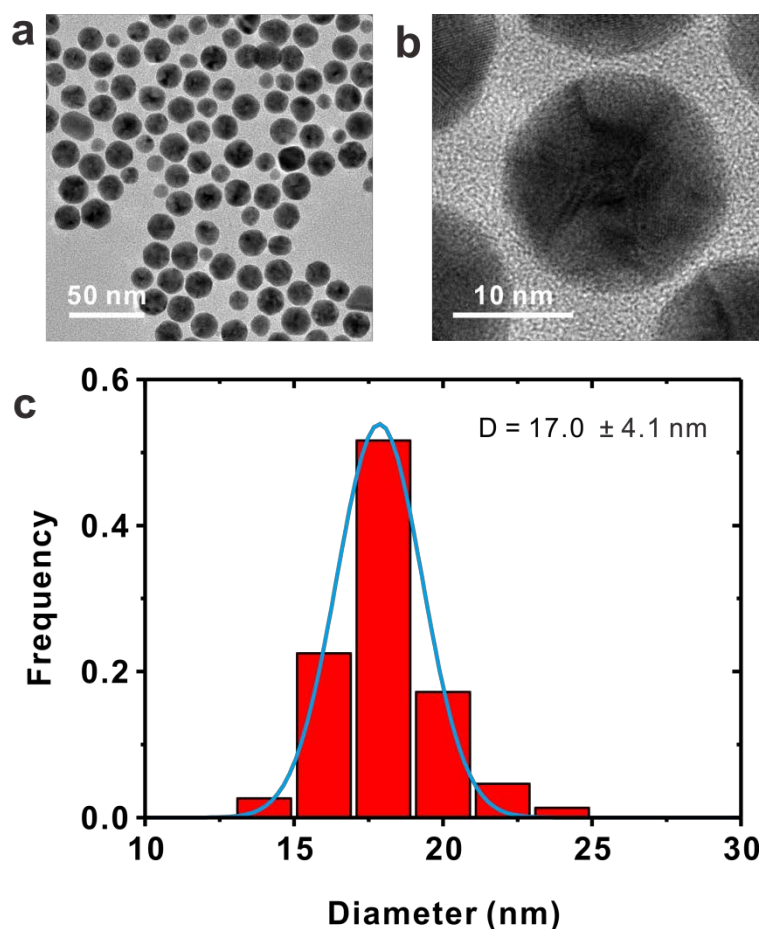


**Figure S1.** (a, b) Representative TEM images and (c) size distribution of Au@DHBC NPs prepared by modified method.<sup>3</sup> Specifically, the DHBC poly(ethylene oxide)-*block*-poly(acrylic acid) (PEO-*b*-PAA) is used as both a template and stabilizer for Au NPs. Typically, the carboxylate group of the PAA block interacts with the Au precursor via coordinative bonding between the metal precursor and the carboxylate group. Then, the PAA blocks segregate to form micellar structures in solution. Once the micelle formation is induced, the PEO-*b*-PAA micelle acts as a nanoreactor to template the growth of the Au NP within the micellar core upon the addition of a reducing agent, L-ascorbic acid. As the Au precursor is reduced to Au NPs, the transparent yellow solution turns reddish, indicating the formation of Au NPs. The average diameter of the Au NPs formed within the DHBC template (Au@DHBC NPs) is  $17.0 \pm 4.1$  nm.

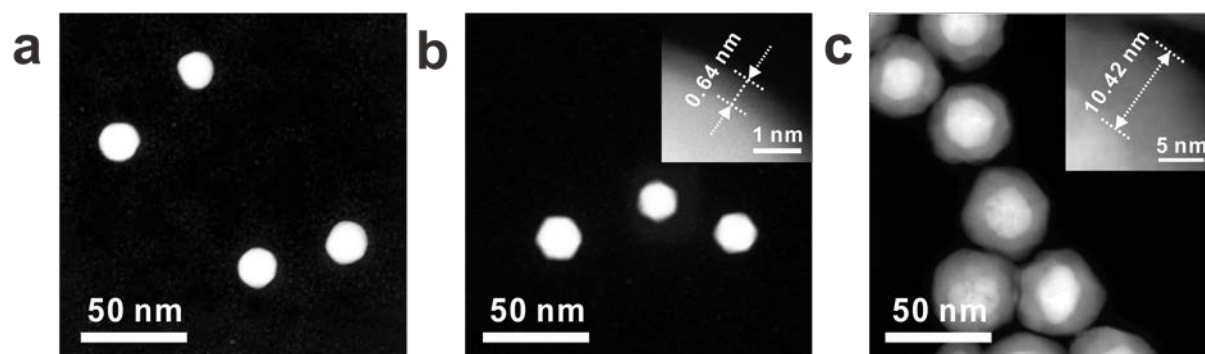


**Figure S2.** Low-magnification dark field HAADF STEM images of (a) Au@DHBC NPs, (b) Au@Ag<sub>0.1</sub>@DHBC NPs, and (c) Au@Ag<sub>0.9</sub>@DHBC NPs. Insets in b and c show the high resolution dark field TEM images of Au@Ag@DHBC NPs.

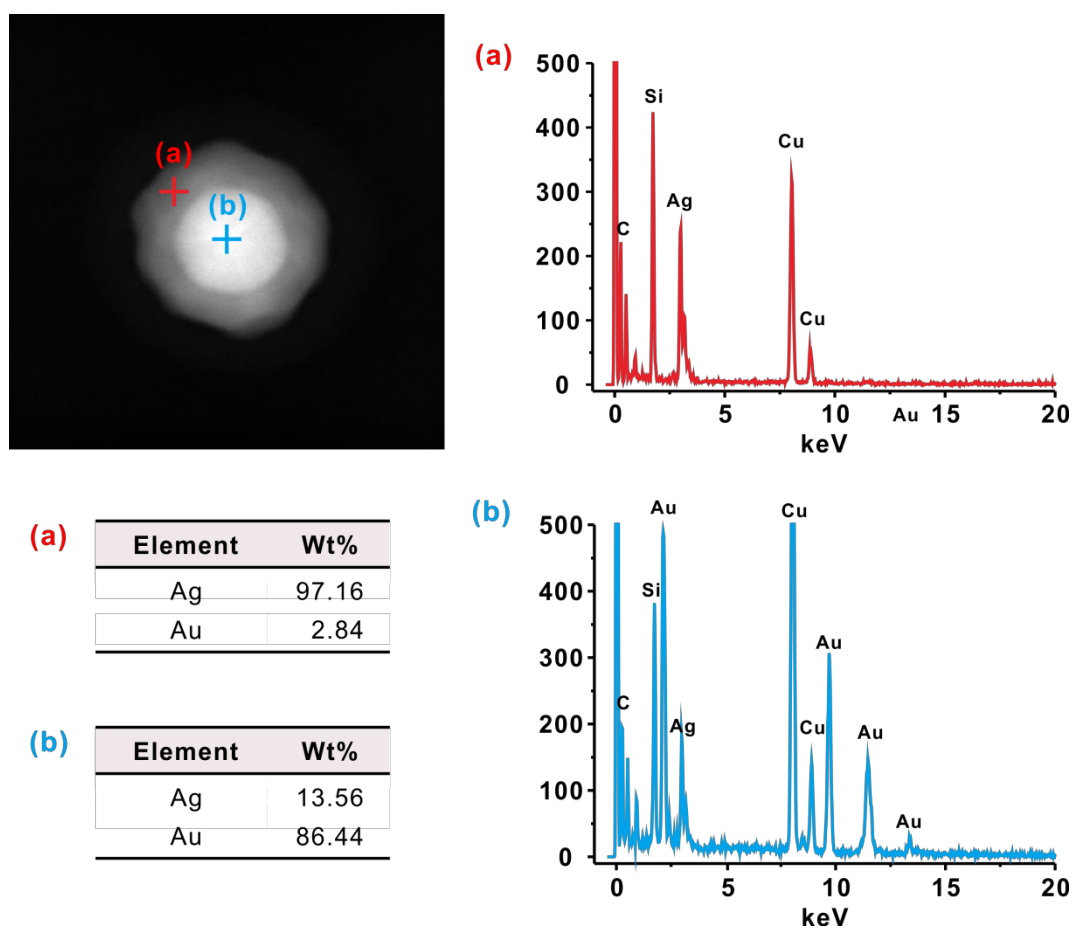


**Figure S3.** STEM analysis of representative Au@Ag@DHBC NPs. (a-b) Energy dispersive X-ray spectroscopy data of core-shell structure showing the component of Au and Ag at the different site of nanoparticles. The other atoms are observed because of the TEM grid.

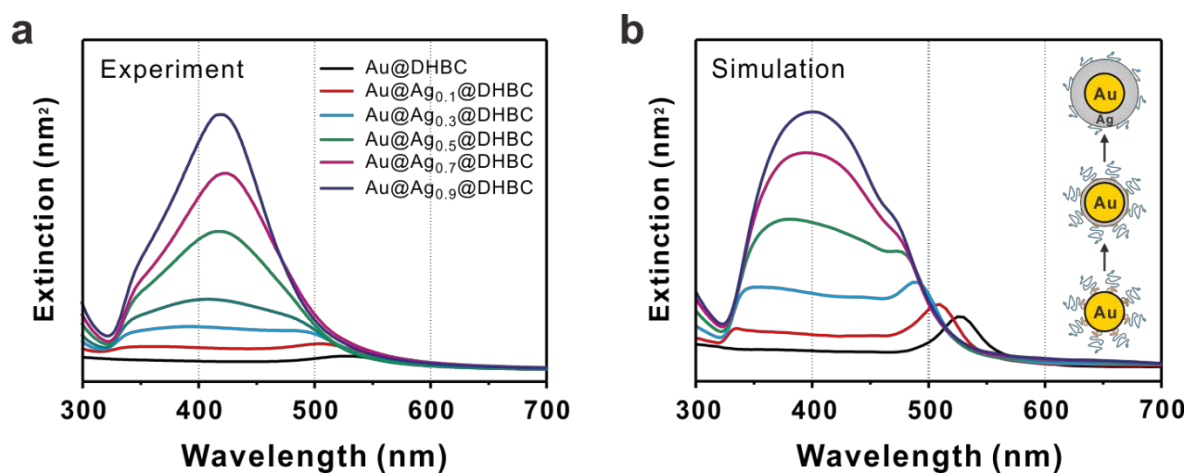


**Figure S4.** A comparison of the (a) UV-Vis spectra and (b) FDTD simulation results collected for Au@Ag<sub>n</sub>@DHBC NPs produced with different concentrations of Ag precursor ( $n = 0.0 - 0.9$ ). The experiment data indicates that the plasmon bands of the NPs initially blue-shifted and then exhibited strong absorption with increasing Ag shell thickness, showing a similar trend as the simulation data.

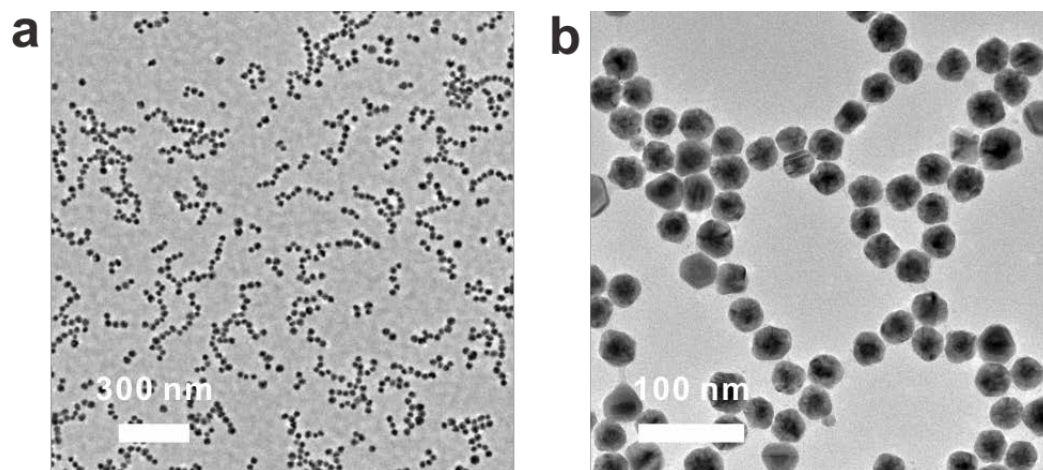


**Figure S5** (a) Low and (b) high-resolution TEM images of Au@Ag<sub>0.9</sub>@DHBC NPs.

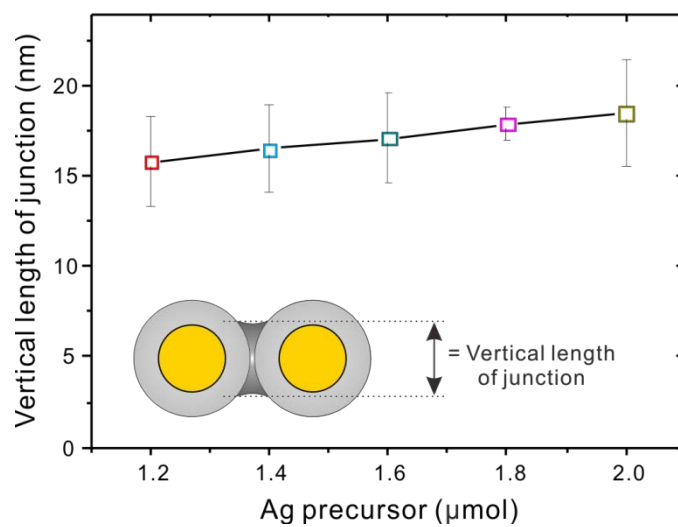


**Figure S6.** The plot showing vertical length of junction formed between NPs as a function of Ag precursor. Inset indicating the area of junction and corresponding vertical length.

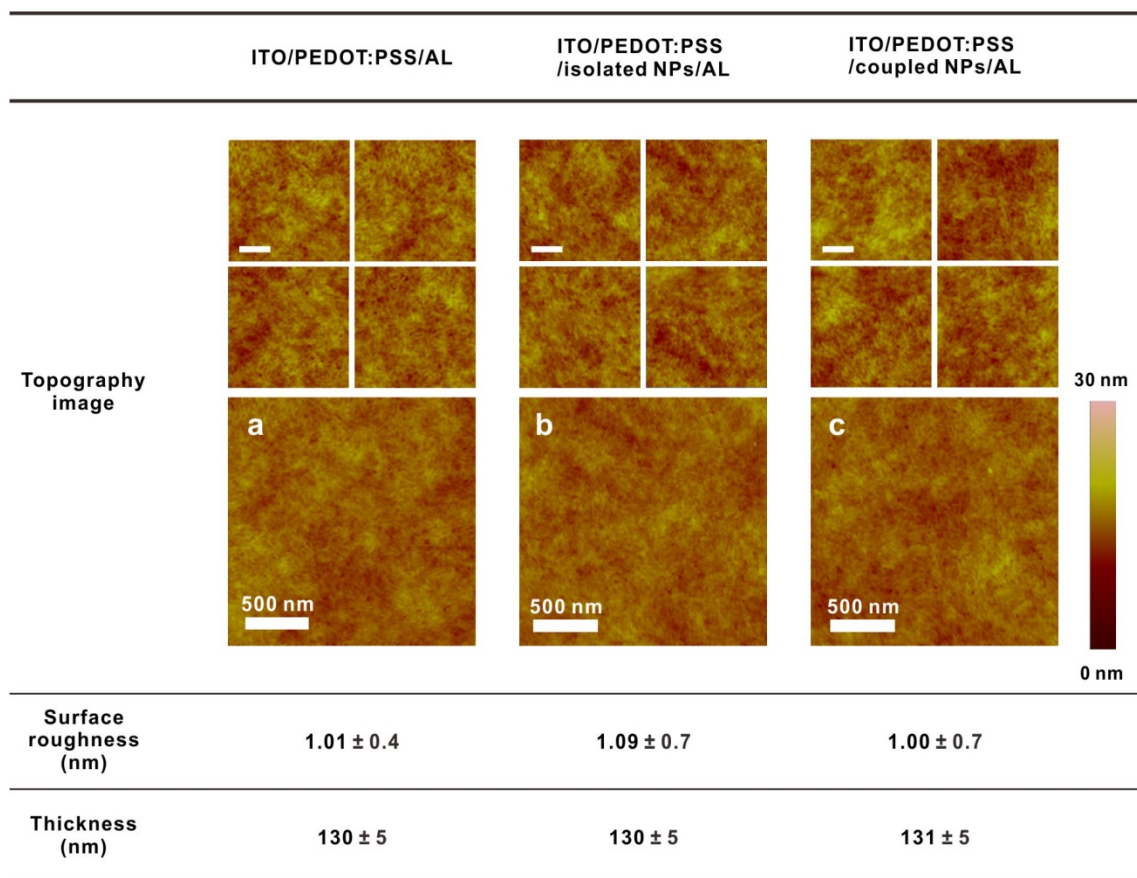


**Figure S7.** AFM images of active layer with configurations of (a) ITO/PEDOT:PSS/active layer, (b) ITO/PEDOT:PSS/isolated NPs/active layer, and (c) ITO/PEDOT:PSS/coupled NPs/active layer. Scale bar in all images represents 500 nm. The thickness of the films was measured with profilometer.

## Supporting Information

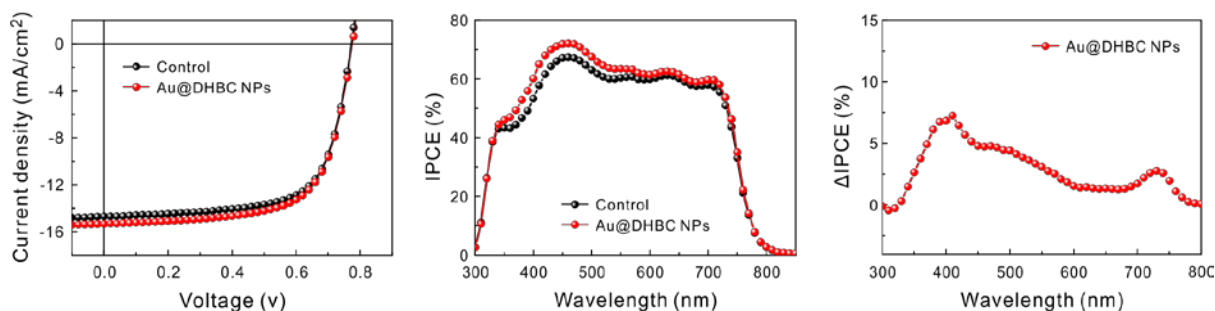


**Figure S8.** Device characteristics and spectral responses of plasmonic PSCs with and without Au@DHBC NPs. (a) Current density-voltage (J-V) characteristics and (b) IPCE of a control device (black circles) and the best plasmonic PSCs with embedded Au@DHBC NPS (red circle). (c) Enhanced IPCE of device with Au@DHBC NPs in comparison with control device.

**Table S1.** Device Characteristics of PTB7-Th:PC<sub>71</sub>BM-based PSCs with Au@DHBC NPs

Device configuration	Plasmonic NPs		$J_{sc}$ (mA/cm <sup>2</sup> )	$V_{oc}$ (V)	FF	PCE (%)	$J_{sc}$ [cal.] (mA/cm <sup>2</sup> )
ITO/PEDOT:PSS/ AL <sup>a</sup> /Al	None (control)	Best	14.53	0.78	0.68	7.77	14.41
		Average	14.12 ± 0.41	0.78 ± 0.00	0.67 ± 0.01	7.37 ± 0.40	
ITO/PEDOT:PSS/ Au@DHBC NPs/AL <sup>a</sup> /Al	Au@DHBC NPs	Best	15.30	0.78	0.67	8.01	15.18
		Average	15.12 ± 0.18	0.77 ± 0.01	0.69 ± 0.00	7.86 ± 0.15	

<sup>a</sup> AL: active layer consisting of PTB7-Th and PC<sub>71</sub>BM

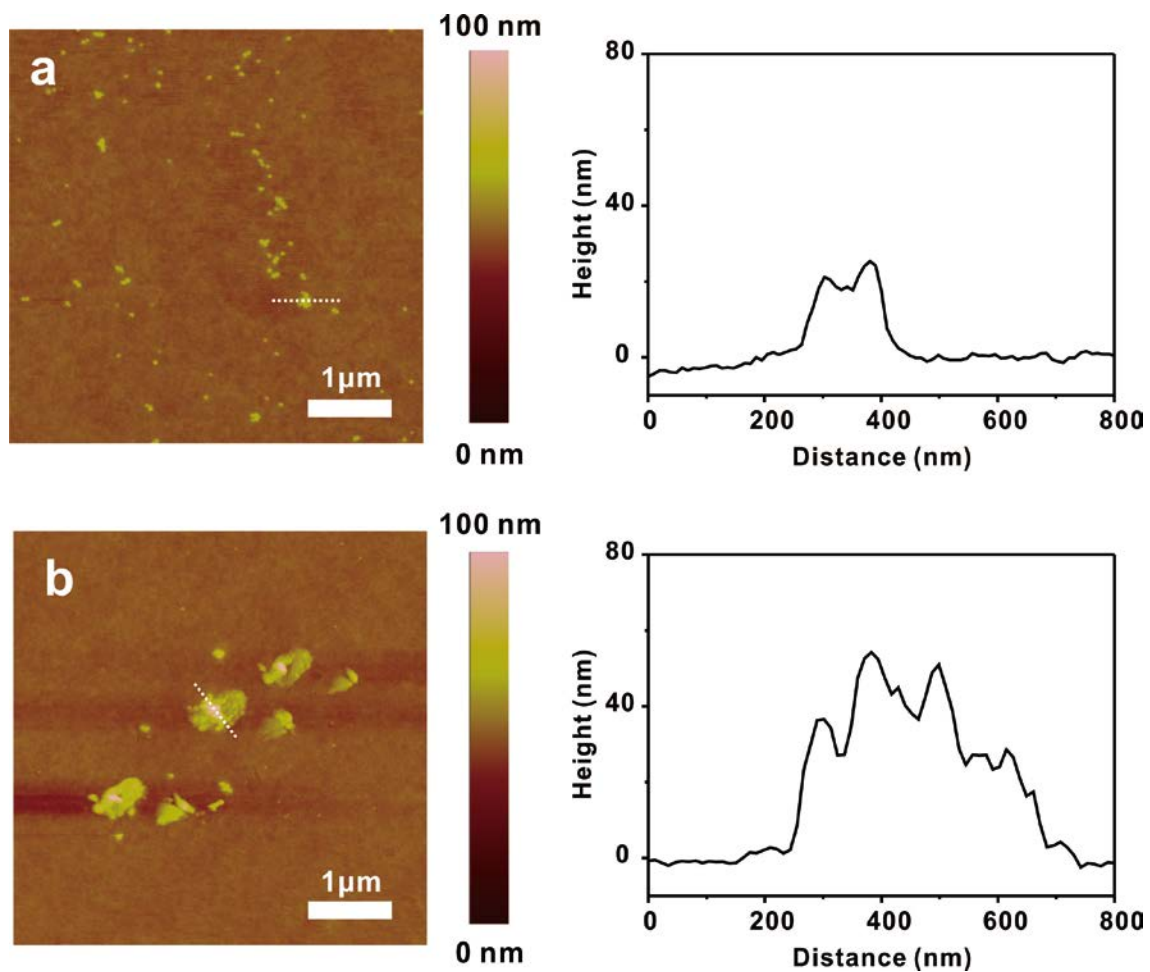


**Figure S9.** Representative height-mode AFM images of PEDOT:PSS film coated with (a) isolated Au@Ag<sub>0.9</sub>@DHBC NPs and (b) coupled Au@Ag<sub>1.6</sub>@DHBC NPs. The images were taken with NPs solutions after filtration.

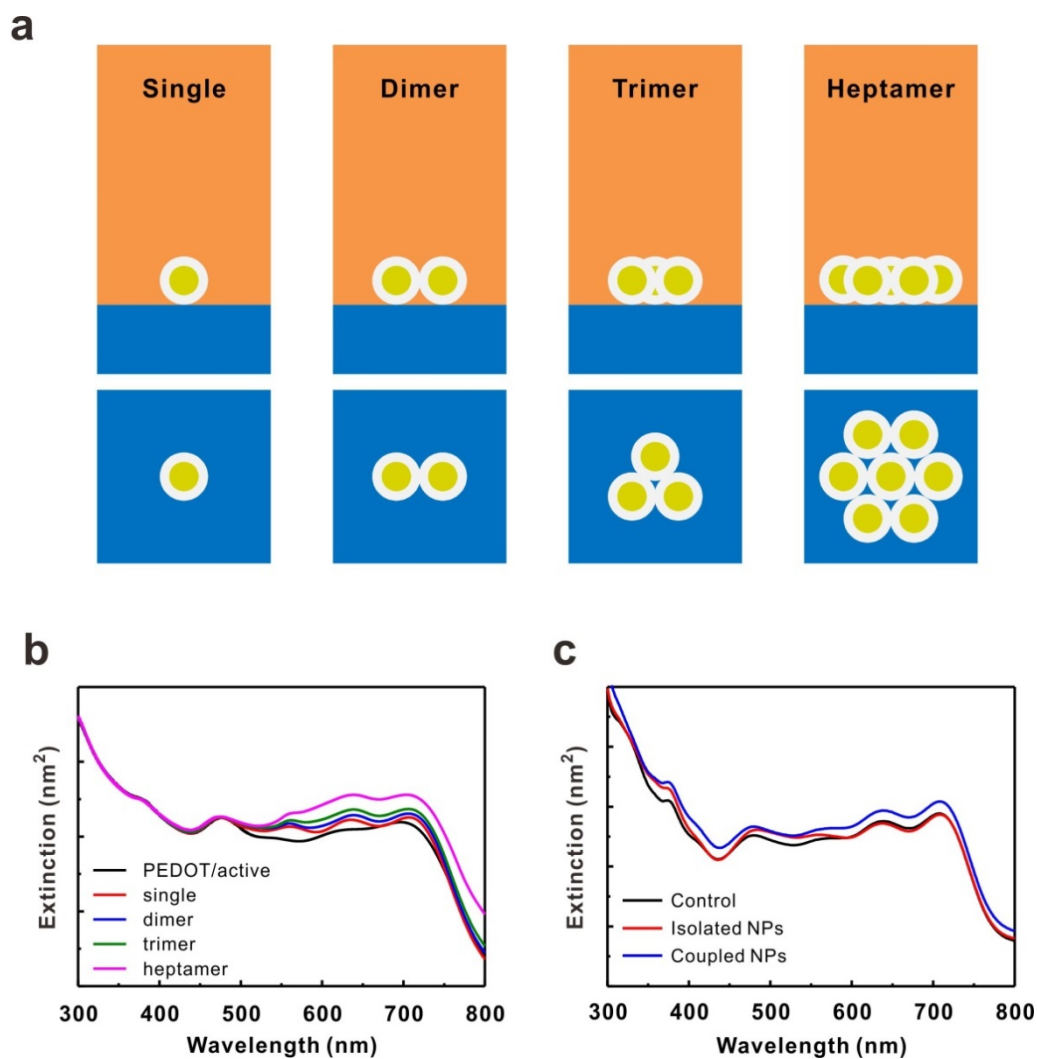


**Figure S10.** (a) Schematic description of different arrangement of plasmonic Au@Ag@DHBC NPs embedded within active layer on the device and (b) corresponding FDTD simulated extinction. (c) UV-Vis spectra of PTB7/PC<sub>71</sub>BM without NPs and with isolated Au@Ag<sub>0.9</sub>@DHBC NPs or coupled Au@Ag<sub>1.6</sub>@DHBC NPs.

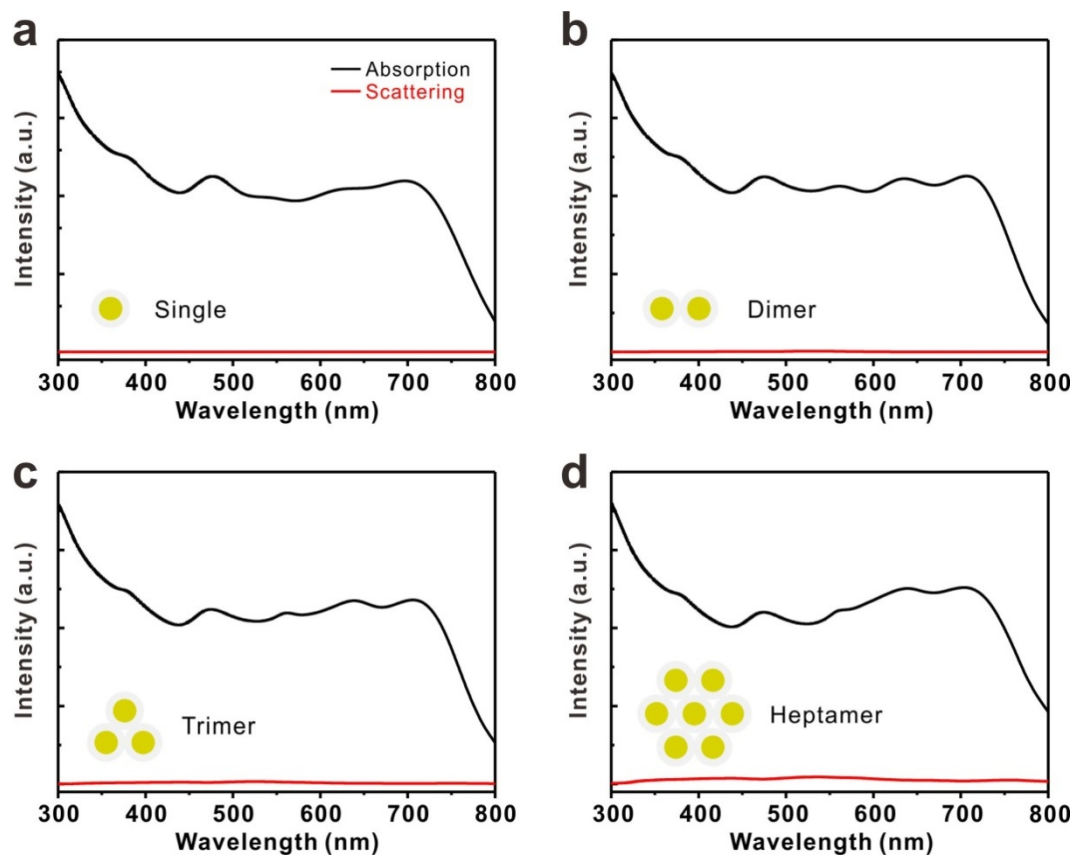


**Figure S11.** The absorption and scattering spectra on the device with plasmonic Au@Ag core-shell NPs, which is analyzed using FDTD simulation.

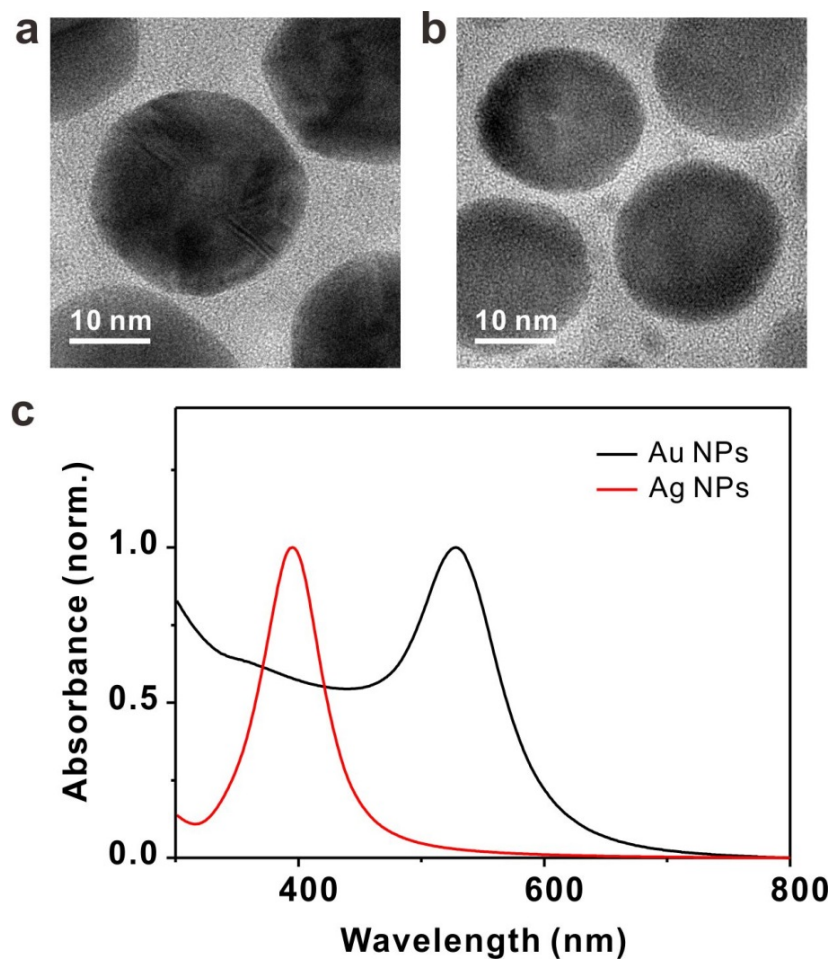


**Figure S12.** (a, b) Representative TEM images of (a) free Au and (b) free Ag NPs without DHBC and (c) normalized UV-vis spectra of Au and Ag NP solutions.

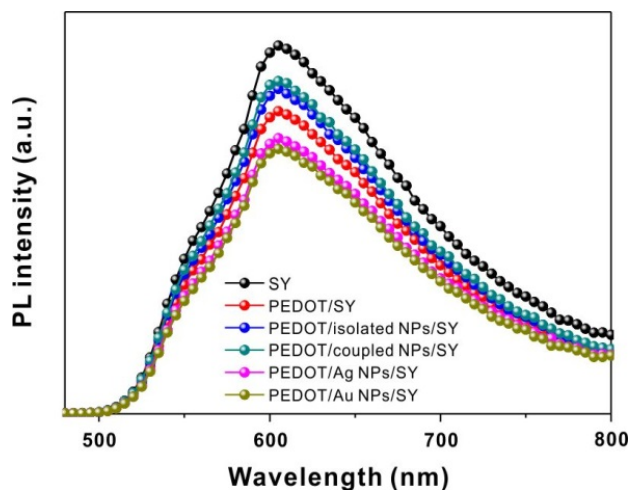


**Figure S13.** Steady-state photoluminescence (PL) spectra of fluorescence of SY films by the effect of isolated and coupled NPs ( $\text{Au@Ag}_{0.9}\text{@DHBC}$  and  $\text{Au@Ag}_{1.6}\text{@DHBC}$  NPs, respectively) and free Au and Ag NPs synthesized without DHBC template.

## References

1. He, J.; Liu, Y.; Babu, T.; Wei, Z.; Nie, Z. Self-Assembly of Inorganic Nanoparticle Vesicles and Tubules Driven by Tethered Linear Block Copolymers. *J. Am. Chem. Soc.* **2012**, *134*, 11342-11345.
2. Jana, N. R.; Gearheart, L.; Murphy, C. J. Seeding Growth for Size Control of 5-40 nm Diameter Gold Nanoparticles. *Langmuir* **2001**, *17*, 6782-6786.
3. Seo, E.; Kim, J.; Hong, Y.; Kim, Y. S.; Lee, D.; Kim, B.-S. Double Hydrophilic Block Copolymer Templated Au Nanoparticles with Enhanced Catalytic Activity toward Nitroarene Reduction. *J. Phys. Chem. C* **2013**, *117*, 11686-11693.